Higgs+Jet at NNLO with Antenna Subtraction Method

Student Seminar

Xuan Chen

Institute for Particle Physics Phenomenology
University of Durham

Durham, November 17, 2014

Higgs Boson: Precision Physics

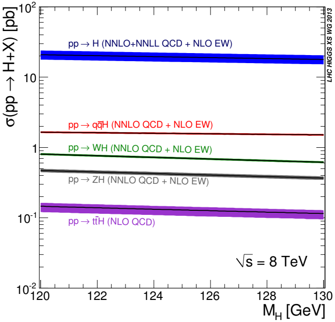

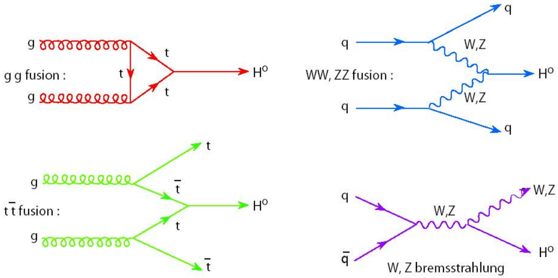

- Higgs discovery requires very sophisticated theory predictions
  - Higer-order perturbative calculations
  - Resummation program
  - Reliable non-perturbative tools (PDFs, PS, Jet structure ...)
- BSM effects are well hidden → more precise study of Higgs couplings

Higgs Boson: Cutting Edge Predictions

- Higgs production: testing the edge of pQCD
  - Theoretical uncertainty is expected around 5%
  - N^3LO pp$\to$ H towards the full result (second term in threshold expansion) Anastasiou, Duhr et al (14)
  - Approximation from resummation Bonvini, Ball et al (13,14); De Florian, Mazzitelli et al (14)
- Higgs + jets final states: jet-bin analysis, differential cross section
  - Critical to test Higgs couplings and properties
  - Resumming jet vetoes Stewart,Tackmann et al; Banfi, Monni et al (13)
  - Higgs+Jet @ NNLO Boughezal, Caola et al (13); Chen, Gehrmann et al (14)
  - Higgs+Jets @ NLO MCFM, Sherpa, GoSam, aMC@NLO, POWHEG, MadLoop
- Improving above tools:
  - Finite m_t, m_b correction Harlander et al, (12); Grazzini, Sargsyan (13)
  - Parton shower (PS) matching @ NNLO Hamilton, Nason et al (13)
  - NNPDF for LHC Run II Ball, Bertone et al (14)

Higgs + jets: jet bin analyses in LHC

- $pp \to H \to \gamma\gamma$

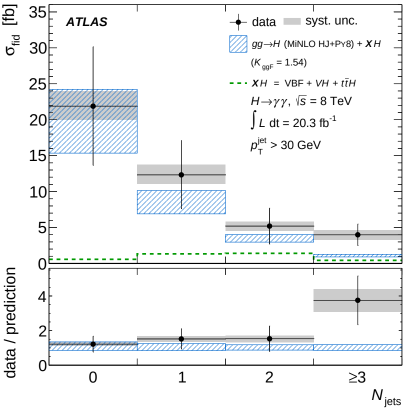

- $pp \to H \to ZZ^*$

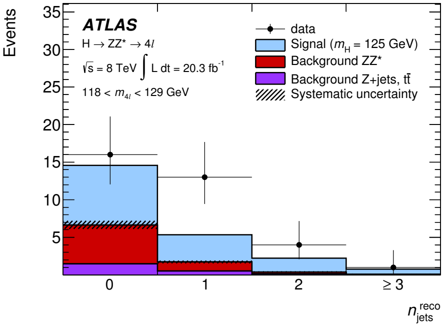

- Different Signal/Background ratio for each bin
- Large theory error in high jet multiplicity
- Different experimental challenge in parameter space

Higgs + jets: jet bin analyses in LHC

- $pp \to H \to WW^{(*)}$

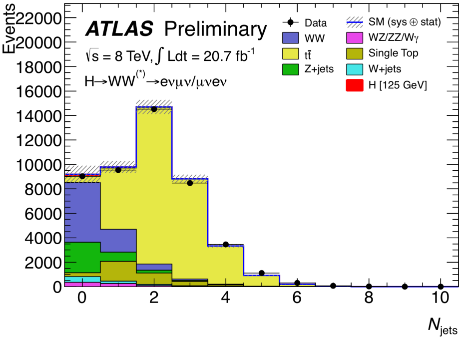

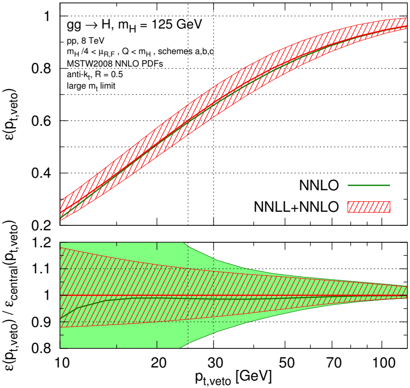

Banfi et al (12,13); Tackmann et al (12,13)

- Various selection rules in experiment to distinguish signal from background
- Need to study the precise theory involving those selection rules (e.g. jet veto cut)
  - 0-jet bin: $\sigma_0 = \sigma_{tot} - \sigma_{\geq 1}$
  - Unertainty can be reduced by improving $\sigma_{\geq 1}$

Higgs + jets: Differential cross section in LHC

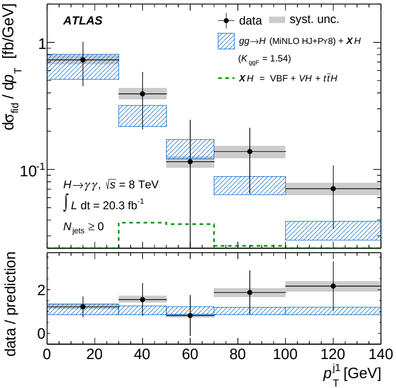

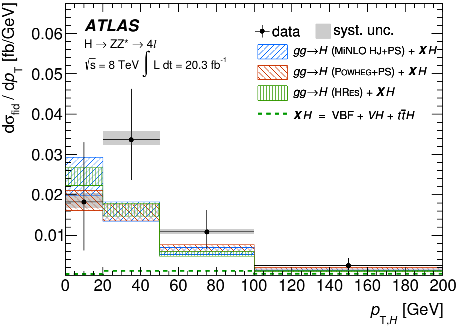

- Differential corss sections contain detailed properties of Higgs
- Large prediction error dominate by missing higher orders
- Request for more precise differential predictions

Higgs+jet @ NNLO in gluon fusion

- Independent computation of gg $\rightarrow$ H + J at NNLO in HEFT using Antenna Subtraction method
    - Computation for 8TeV LHC
    - Fully differential cross section
    - VEGAS integration coded up in FORTRAN
    - Dedicated phasespace generator
    - k_T with R=0.5, P_T cut at 30GeV
    - Use NNPDF23 set
    - Fixed central scale $\mu_R = \mu_F = M_H$
- One of the first NNLO processes done with two different subtraction formalisms
    - gg $\rightarrow$ H + J Sector-improved decomposition subtraction. Boughezal, Caola, Melnikov, Petriello, Schulze 1302.6216 [hep-ph] (cross section)
    - gg $\rightarrow$ H + J Antenna subtraction. Chen, Gehrmann, Glover and Jaquier 1408.5325 [hep-ph] (differential distribution)
    - Important crosscheck

Higgs+jet @ NNLO in gluon fusion

- Importance of other channels

Cross section @ LO (pb)					
Process	30 GeV	50 GeV	100 GeV	150 GeV	200 GeV
$gg \to gH$	7.6	4.2	1.4	0.67	0.35
$pg \to pH$	9.9	6.1	2.8	1.8	1.4
$pp \to gH$	7.7	4.2	1.5	0.68	0.35
Cross section branch ratio @ LO					
Process	30 GeV	50 GeV	100 GeV	150 GeV	200 GeV
$gg \to gH$	75.9%	69%	52.2%	36.7%	24.6%
$qg \to qH$	23.3%	30.2%	47.2%	62.7%	74.9%
$qq \to gH$	0.8%	0.8%	0.6%	0.6%	0.5%

- Madgraph 5: fixed scale $\mu_R = \mu_F = M_H$, 0.1 million events, 13 TeV CME
- Vary jet cuts for the leading jet (30, 50, 100, 150, 200 GeV)
- gg and qg initiated channel dominant with qg the most important at high P_T

Higgs+jet building blocks

- Higgs production via gluon fusion through a quark loop. In the heavy Top mass limit, we have the effective interaction

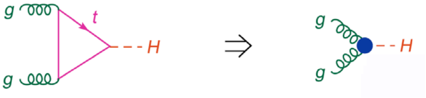

- The effective interaction term in Lagrangian Wilczek, Shifman et al (70's)

$$\mathcal{L}_H^{int} = \frac{C}{2} H \ \mathrm{Tr} G_{\mu\nu} G^{\mu\nu}$$

$$C = \frac{\alpha_s}{6\pi V}(1 + \mathcal{O}(\alpha_s))$$

- Heavy Top quark mass limit gives less than 1% theoretical uncertainty Harlander, Mantler et al (10)

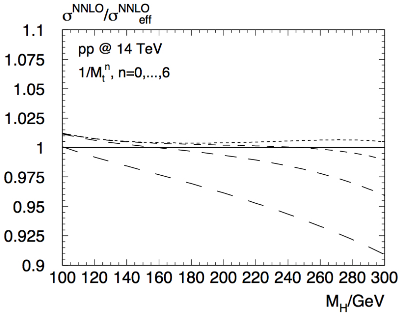

- Heavy Top mass limit approximation breaks down in high P_T region Harlander, Neumann et al (12)

Higgs+jet building blocks

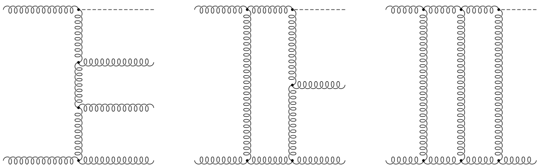

- tree level 2→3+H amplitudes Del Duca, Frizzo, Maltoni; (use BCFW) Chen;
  - Implicit divergency in P.S. (IR)
- 1-loop 2→2+H amplitudes Berger, Del Duca, Dixon; Badger, Glover, Mastrolia, Williams; Badger, Ellis
  - Implicit divergency in P.S. (IR) as well as explcit poles up to ϵ^{-2} (UV)
- 2-loop 2→1+H amplitudes Gehrmann, Jaquier, Glover, Koukoutsakis
  - Explicit poles up to ϵ^{-4} (UV)
- Analytic results with spinor-helicity formalism (stable check in unresolved P.S.)

Higgs+jet building blocks

- tree level scattering amplitudes in QCD
  - MHV amplitudes (certain helicity) Parke, Taylor (86)
  - Twistor string theory (geometrical interpretation of MHV amplitudes) Witten (03)
  - CSW amplitudes (all helicity off-shell recursion) Cachazo, Svrcek and Witten (04)
  - BCFW amplitude (on-shell recursion) Britto,Cachazo,Feng and Witten (05)
  - CHY formular (based on KLT Orthogonality, Yang-Mills and gravity theories in arbitrary spacetime dimensions) Cachazo,He, and Yuan (14)
  - Ambitwistor string theory (high energy string scattering) Mason, Skinner (14)
- 1-loop scattering amplitudes in QCD
  - Unitarity-based recursive method (on-shell cut for loop, recycle BCFW amplitudes) Berger, Bern, Dixon, Forde, Kosower (06)
  - Use $\mathcal{N} = 4$ Super-Yang-Mills QCD properties.
  - Rational piece in the finite contribution not fully recovered.
- 2-loop scattering amplitudes in QCD
  - Currently still based on Feynman rules

Parton Level Cross Section Structure at NNLO

$$
\begin{aligned}
d\hat{\sigma}_{NNLO} &= \int [\langle \mathcal{M}^0 | \mathcal{M}^0 \rangle]_{H+5} d\Phi_{H+3} \\
&+ \int [\langle \mathcal{M}^0 | \mathcal{M}^1 \rangle + \langle \mathcal{M}^1 | \mathcal{M}^0 \rangle]_{H+4} d\Phi_{H+2} \\
&+ \int [\langle \mathcal{M}^1 | \mathcal{M}^1 \rangle + \langle \mathcal{M}^2 | \mathcal{M}^0 \rangle + \langle \mathcal{M}^0 | \mathcal{M}^2 \rangle]_{H+3} d\Phi_{H+1} \\
&= \int_{d\Phi_{H+3}} d\hat{\sigma}^{RR}_{NNLO} + \int_{d\Phi_{H+2}} d\hat{\sigma}^{RV}_{NNLO} + \int_{d\Phi_{H+1}} d\hat{\sigma}^{VV}_{NNLO}
\end{aligned}
$$

- $d\hat{\sigma}$ renormalised factorized parton level cross section
- Analytical integration of P.S. transforms IR divergence into explicit poles
- Challenge to extract implicit IR divergence from RR and RV without P.S. integration
  - Calculate RR and RV in separate parton level Monte Carlos
  - Collect finite contributions from RR and RV for differential cross-section analysis

NNLO Subtraction

$$
\begin{aligned}
d\hat{\sigma}_{NNLO} = & \int_{d\Phi_{H+3}} \left(d\hat{\sigma}^{RR}_{NNLO} - d\hat{\sigma}^{S}_{NNLO} \right) \\
& + \int_{d\Phi_{H+2}} \left(d\hat{\sigma}^{RV}_{NNLO} - d\hat{\sigma}^{T}_{NNLO} \right) \\
& + \int_{d\Phi_{H+1}} \left(d\hat{\sigma}^{VV}_{NNLO} - d\hat{\sigma}^{U}_{NNLO} \right)
\end{aligned}
$$

- Subtraction terms mimic the divergent behaviour of matrix elements
- Each bracket is finite
- Calculations in d dimension for explicit pole cancellation
- The construction of red terms and the treatment of P.S. depends on the subtraction method
  - Antenna Subtraction
  - Sector-Improved Decomposition Subtraction

- Consistency requirement:

$$
0 = \int_{d\Phi_{H+3}} d\hat{\sigma}^{S}_{NNLO} + \int_{d\Phi_{H+2}} d\hat{\sigma}^{T}_{NNLO} + \int_{d\Phi_{H+1}} d\hat{\sigma}^{U}_{NNLO}
$$

Antenna Subtraction Method

Gehrmann-De Ridder, Gehrmann, Glover

- Subtraction terms constructed from antenna functions (from ME)
- Each antenna has two specified hard radiators + 1 or 2 unresolved patrons

$$X_3^0(i,j,k) \sim \frac{|\mathcal{M}_{ijk}^0|^2}{|\mathcal{M}_{IL}^0|^2}$$

$$X_4^0(i,j,k,l) \sim \frac{|\mathcal{M}_{ijkl}^0|^2}{|\mathcal{M}_{IL}^0|^2}$$

$$X_3^1(i,j,k) \sim \frac{|\mathcal{M}_{ijk}^1|^2}{|\mathcal{M}_{IK}^0|^2} - X_{ijk}^0 \frac{|\mathcal{M}_{IK}^1|^2}{|\mathcal{M}_{IK}^0|^2}$$

- Momentum mappings give the P.S. for reduced ME

$$d\Phi_{H+3} \rightarrow d\Phi_{H+2}$$
$$d\Phi_{H+3} \rightarrow d\Phi_{H+1}$$
$$d\Phi_{H+2} \rightarrow d\Phi_{H+1}$$

- Integrated antenna functions all known and contain explicit poles
- Explicit pole cancellation between integrated antenna functions and loop calculations is analytical

Antenna Subtraction Method

- Antenna function form physical matrix elements

$$A,\ \widetilde{A},\ B,\ C\ \sim\ \gamma^* \to q\bar{q}\ + partons\ (hard\ quark - antiquark\ pair)$$
$$D,\ E,\ \widetilde{E}\ \sim\ \widetilde{\mathcal{X}} \to \tilde{g}\ + partons\ (hard\ quark - gluon\ pair)$$
$$F,\ G,\ \widetilde{G},\ H\ \sim\ H \to\ partons\ (hard\ gluon - gluon\ pair)$$

Gehrmann-De Ridder, Gehrmann, Glover, 05

- Complete set of Antenna tool box

$$phase\ config. \otimes type \otimes parton\ types$$
$$[FF, IF, II] \otimes [X_3^0, X_4^0, X_3^1] \otimes [A \sim H]$$

- All antenna functions are analytically integrable
  - Final-Final $\mathcal{X}_3^0$, $\mathcal{X}_4^0$ and $\mathcal{X}_3^1$ Gehrmann-De Ridder, Gehrmann, Glover (05)
  - Initial-Final $\mathcal{X}_3^0$, $\mathcal{X}_4^0$ and $\mathcal{X}_3^1$ Daleo, Gehrmann, Gehrmann-De Ridder, Luisoni, Maitre (06,09,12)
  - Initial-Initial $\mathcal{X}_3^0$, $\mathcal{X}_4^0$ and $\mathcal{X}_3^1$ Boughezal, Daleo, Gehrmann-De Ridder, Gehrmann, Maitre, Monni, Ritzmann (10,11,12)

Antenna subtraction for double real emission (RR)

$$d\hat{\sigma}^{S}_{NNLO} \sim X_3^0|\mathcal{M}^0_{n+1}|^2 + X_4^0|\mathcal{M}^0_n|^2 + X_3^0X_3^0|\mathcal{M}^0_n|^2 + X_3^0|\mathcal{M}^0_n|^2 soft$$

- Three possible colour ordering of double unresolved particles

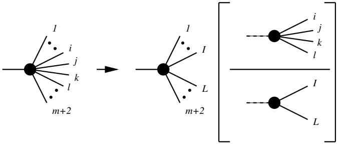

(a) colour connected $X_4^0 \otimes |\mathcal{M}^0_n|^2$

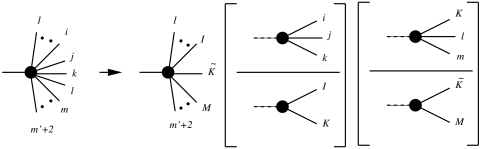

(b) colour almost connected $X_3^0 \otimes X_3^0 \otimes |\mathcal{M}^0_n|^2$

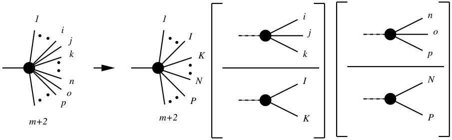

(c) colour not connected $X_3^0 \otimes X_3^0 \otimes |\mathcal{M}^0_n|^2$

Antenna subtraction for double real emission (RR)

$$d\hat{\sigma}^{S}_{NNLO} \sim X_3^0|\mathcal{M}^0_{n+1}|^2 + X_4^0|\mathcal{M}^0_n|^2 + X_3^0X_3^0|\mathcal{M}^0_n|^2 + X_3^0|\mathcal{M}^0_n|^2 soft$$

- Test structure

$$R = \frac{d\hat{\sigma}^{RR}_{NNLO}}{d\hat{\sigma}^{S}_{NNLO}}$$

- R ~horizontal axis (centre at one near the unresolved region)
- Number of P.S. points in each bin ~ vertical axis
- Controlling singular region to achieve spike plot

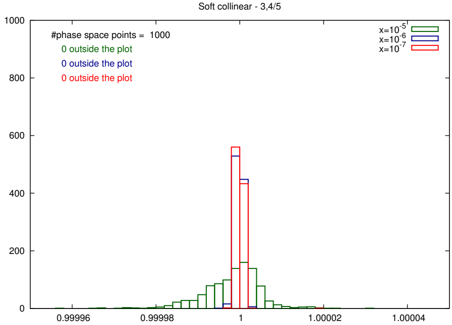

Antenna subtraction for real emission at loop level (RV)

$$d\hat{\sigma}^T_{NNLO} \sim J_2^{(1)}|\mathcal{M}^0_{n+1}|^2 + X_3^0|\mathcal{M}^1_n|^2 + X_3^1|\mathcal{M}^0_n|^2 + J_2^{(1)}X_3^0|\mathcal{M}^0_n|^2$$

Currie, Glover, Wells (13)

- Only single unresolved limit

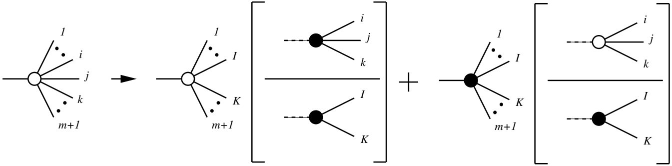

(d) Loop level: $X_3^0|\mathcal{M}^1_n|^2 + X_3^1|\mathcal{M}^0_n|^2$

$$J_2^{(1)} = \int X_3^0 d\Phi_{FF,IF,II} + M.F._{IF,II}$$

$$Poles\left(J_{2,ij}^{(1)}\right) = Poles\left(I_{ij}^{(1)}(\epsilon, s_{ij})\right)$$

Antenna subtraction for real emission at loop level (RV)

$$d\hat{\sigma}^{T}_{NNLO} \sim J_2^{(1)}|\mathcal{M}^0_{n+1}|^2 + X_3^0|\mathcal{M}^1_n|^2 + X_3^1|\mathcal{M}^0_n|^2 + J_2^{(1)}X_3^0|\mathcal{M}^0_n|^2$$

- Single unresolved limits preserve both explicit and implicit pole cancellation

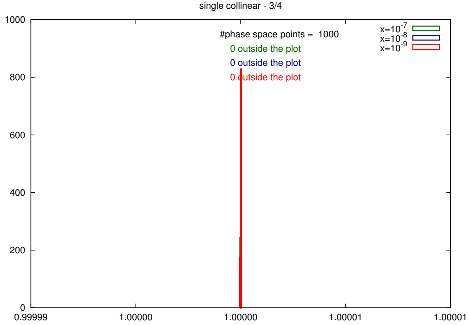

Figure : $\frac{1}{\epsilon^2}$ & $\frac{1}{\epsilon}$ pole

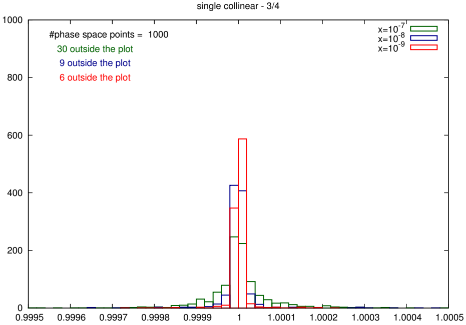

Figure : ϵ^0 pole

Antenna subtraction for two-loop level (VV)

- Double virtual level only have explicitly poles and no parton become unresolved
- Collect all leftover subtraction terms (integrated) in $d\hat{\sigma}^{U}_{NNLO}$

$$
\begin{aligned}
d\hat{\sigma}^{U}_{NNLO} \sim\ & J_2^{(1)}(|\mathcal{M}_n^1|^2 - \frac{\beta_0}{\epsilon}|\mathcal{M}_n^0|^2) \\
& - \frac{1}{2} J_2^{(1)} \otimes J_2^{(1)} |\mathcal{M}_n^0|^2 \\
& + J_2^{(2)} |\mathcal{M}_n^0|^2
\end{aligned}
$$

Currie, Glover, Wells (13)

$$
pole\{d\hat{\sigma}^{VV}_{NNLO}\} \sim pole\left\{ I_{ij}^{(1)} \otimes |\mathcal{M}_n^1|^2 - (\frac{1}{2} I_{ij}^{(1)} \otimes I_{ij}^{(1)} + \frac{\beta_0}{\epsilon} - I_{ij}^{(2)})|\mathcal{M}_n^0|^2 \right\}
$$

S. Catani (98)

- VV pole cancellation analytically checked with FORM
- Master code (.map) $\rightarrow$ (.frm) (.f) (.tex)

Higgs+jet @ NNLO in gluon fusion

- Independent computation of gg → H + J at NNLO in HEFT using Antenna Subtraction method
  - Computation for 8TeV LHC
  - Fully differential cross section
  - VEGAS integration coded up in FORTRAN
  - Dedicated phasespace generator
  - k_T with R=0.5, P_T cut at 30GeV
  - Use NNPDF23 set
  - Fixed central scale $\mu_R = \mu_F = M_H$
- One of the first NNLO processes done with two different subtraction formalisms
  - gg → H + J Sector-improved decomposition subtraction. Boughezal, Caola, Melnikov, Petriello, Schulze 1302.6216 [hep-ph] (cross section)
  - gg → H + J Antenna subtraction. Chen, Gehrmann, Glover and Jaquier 1408.5325 [hep-ph] (differential distribution)
  - Important crosscheck

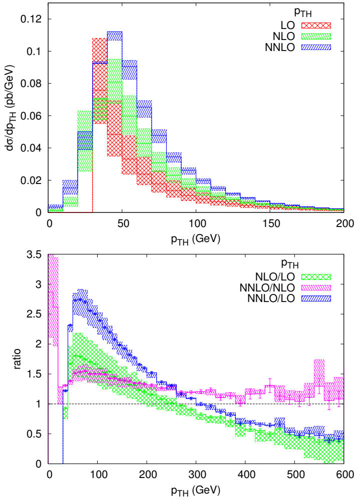

- NLO changes normalisation + shape compare to LO
- NNLO changes normalisation (∼1.4), but changes shape less compared to NLO
- Sizeable NNLO corrections throughout whole P_{TH} range
- Real radiation gives contribution to P_{TH} at $P_{TH} < P_T^{cut}$
- Bands show the scale variation between $M_H/2$ and $2M_H$
- Error bars are the numerical integration errors

Chen, Gehrmann, Glover and Jaquier 1408.5325 [hep-ph]

Jet P_T distribution

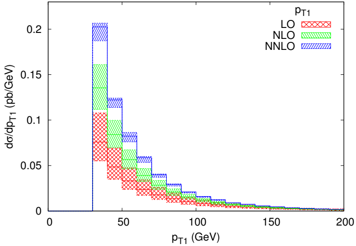

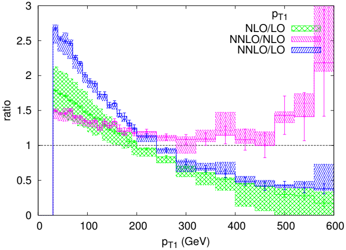

- NLO changes normalisation + shape compare to LO
- NNLO changes normalisation, but changes shape less compare to NLO
- Sizeable NNLO corrections throughout whole P_{TH} range
- At $p_T > m_t$, effective theory for Hgg vertex breaks down. NLO study in 1206.0157 [hep-ph]
- Larger NNLO corrections in higher P_T region
    - Observed cancellation between gg and qg channel in NLO (not complete yet)
    - Illustrate the integrator is well-behaved also at high P_T
- Dynamic scale choice will further improve the current fixed scale result

Chen, Gehrmann, Glover and Jaquier 1408.5325 [hep-ph]

Higgs pseudorapidity distribution

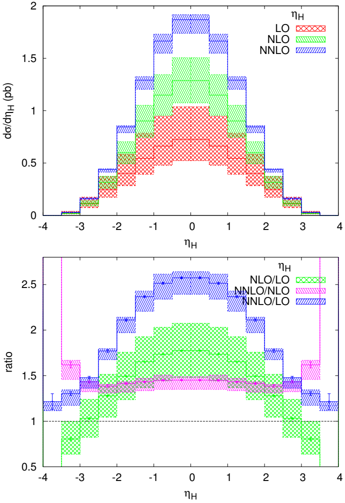

- NLO changes normalisation + shape compare to LO
- NNLO changes normalisation, but changes shape less compare to NLO
- Largest NLO corrections at central rapidity, while becoming moderate at larger rapidities
- Jet cut at high rapidity → large momentum flow (testing the applicability of effective theory approximation)
- The residual theory uncertainty at NNLO is quasi constant for about 9%

Chen, Gehrmann, Glover and Jaquier 1408.5325 [hep-ph]

Jet pseudorapidity distribution

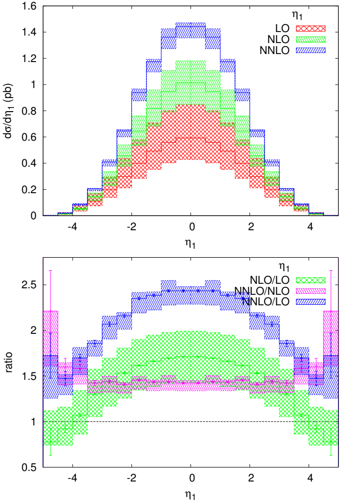

- NLO changes normalisation + shape compare to LO
- NNLO changes normalisation, but changes shape less compare to NLO
- Largest NLO corrections at central rapidity, while becoming moderate at larger rapidities
- Jet cut at high rapidity → large momentum flow (testing the applicability of effective theory approximation)
- The residual theory uncertainty at NNLO is quasi constant for about 9%

Chen, Gehrmann, Glover and Jaquier 1408.5325 [hep-ph]

Summary

- gg channel Higgs + jet @ NNLO
  - Fully differential Higgs + jet cross section at hardon colliders @ NNLO
  - Substantial NNLO corrections in the transverse momentum and rapidity distributions of the Higgs
  - Bring Higgs + jet production to the same level of theory accuracy as inclusive Higgs production
- Future work
  - Prority to compare with ATLAS $H + J \to \gamma\gamma + J$ results (and other possible decay channel)
  - Implement multi-scale ($\mu_R \neq \mu_F$) and dynamic scale ($\mu = \sqrt{m_H^2 + P_{TH}^2}$)
  - Differential cross section for centre of mass energies.
  - qg and qq initiated channels (qg channel dominant in high P_T)

Back up slides

Computation Performance

channel	cross section [pb]	approx. processor time	core	events
$Born$	1.9424 $\pm$ 0.0004	1 min	2	2M
$Virt$	2.8857 $\pm$ 0.0003	30 min	2	2M
$Real$	-0.5720 $\pm$ 0.0022	3 h	10	20M
VV	3.1032 $\pm$ 0.0010	2 min	2	20M
RV	-1.1616 $\pm$ 0.0077	350 h + 1 day warmup	20	40M
RRA	0.0941 $\pm$ 0.0241	1400 h + 5 day warmup	100	500M
RRB	0.0505 $\pm$ 0.0161	1200 h + 5 day warmup	100	250M